JOURNAL OF APPLIED PHYSICS **119**, 134307 (2016)

A new regime of Pauli-spin blockade

Justin K. Perron,[1,2,3,a)] M. D. Stewart, Jr.,[3] and Neil M. Zimmerman[3,b)]
[1]*Department of Physics, California State University San Marcos, California 92096, USA*
[2]*Joint Quantum Institute, National Institute of Standards and Technology, Gaithersburg, Maryland 20899, USA*
[3]*National Institute of Standards and Technology, Gaithersburg, Maryland 20899, USA*

(Received 25 September 2015; accepted 23 March 2016; published online 7 April 2016)

Pauli-spin blockade (PSB) is a transport phenomenon in double quantum dots that allows for a type of spin to charge conversion often used to probe fundamental physics such as spin relaxation and singlet-triplet coupling. In this paper, we theoretically explore Pauli-spin blockade as a function of magnetic field B applied parallel to the substrate. In the well-studied low magnetic field regime, where PSB occurs in the forward $(1, 1) \rightarrow (0, 2)$ tunneling direction, we highlight some aspects of PSB that are not discussed in detail in existing literature, including the change in size of both bias triangles measured in the forward and reverse biasing directions as a function of B. At higher fields, we predict a crossover to "reverse PSB" in which current is blockaded in the reverse direction due to the occupation of a spin singlet as opposed to the traditional triplet blockade that occurs at low fields. The onset of reverse PSB coincides with the development of a tail like feature in the measured bias triangles and occurs when the Zeeman energy of the polarized triplet equals the exchange energy in the $(0, 2)$ charge configuration. In Si quantum dots, these fields are experimentally accessible; thus, this work suggests a way to observe a crossover in magnetic field to qualitatively different behavior. © *2016 AIP Publishing LLC*. [http://dx.doi.org/10.1063/1.4945393]

I. INTRODUCTION

Since its discovery, Pauli-spin blockade (PSB)[1] has been a valuable tool for probing fundamental physics. Its use in spin to charge conversion has led to investigations of spin T_1 relaxation times,[2,3] electron spin couplings to lattice nuclear spins,[4] and spin-orbit effects.[5] PSB has also received a lot of attention from the quantum information community due to its use in read-out and initialization of various electron spin states.[6–8] The majority of studies involving PSB have focused on the low magnetic field regime. In this manuscript we investigate the qualitative behavior of PSB at all magnetic fields. In doing so, we identify experimentally accessible regimes where PSB has yet to be studied and new physics is likely to be found.

In a typical double quantum dot (DQD) device, two quantum dots are coupled to each other as well as to two electron reservoirs (see Figure 1(a)). The dots are also capacitively coupled to one or more gate electrodes which can be used to control the dot potentials. The charge configuration of the system is characterized by a pair of numbers (n, m) corresponding to the number of electrons on the left and right dot, respectively. Transport through quantum dots can be understood by considering the chemical potentials of the quantum dots, $\mu_l(n,m) \equiv E(n,m) - E(n-1,m)$ and $\mu_r(n,m) \equiv E(n,m) - E(n,m-1)$, where E denotes the total energy of the system. When the appropriate chemical potentials form a energetically downhill path between the Fermi levels of the two leads, $\mu_{LL(RL)}$, electron tunnelling through the device is energetically favorable and leads to current flow.[9] Near the $(1, 1) \leftrightarrow (0, 2)$ charge transition, where PSB typically occurs, this condition can be expressed as $\mu_{LL} \geq \mu_l(1,1) \geq \mu_r(0,2) \geq \mu_{RL}$ for transport in the forward $(1, 1) \rightarrow (0, 2)$ direction and $\mu_{LL} \leq \mu_l(1,1) \leq \mu_r(0,2) \leq \mu_{RL}$ for transport in the reverse $(0, 2) \rightarrow (1, 1)$ direction. These conditions describe regions of transport known as bias triangles, with sizes proportional to the applied bias voltage, V_{bias}.[9]

II. CONVENTIONAL PSB IN CHEMICAL POTENTIAL SPACE

For a more complete picture of transport through a DQD near the $(1, 1) \leftrightarrow (0, 2)$ charge degeneracy, we now also consider the spin state of the electrons. For transport in the forward (left to right) direction, current flows via tunneling events that cycle through the $(0,1) \rightarrow (1,1) \rightarrow (0,2) \rightarrow (0,1)$ charge configurations. In the reverse direction, it occurs via $(0,1) \rightarrow (0,2) \rightarrow (1,1) \rightarrow (0,1)$. The two electrons on the DQD can form one of four possible spin states, the $s=0$ spin singlet $|S\rangle \equiv (|\uparrow\downarrow\rangle - |\downarrow\uparrow\rangle)/\sqrt{2}$, or one of the three $s=1$ triplet states $|T_0\rangle \equiv (|\uparrow\downarrow\rangle + |\downarrow\uparrow\rangle)/\sqrt{2}$, $|T_+\rangle \equiv |\uparrow\uparrow\rangle$, $|T_-\rangle \equiv |\downarrow\downarrow\rangle$. In zero magnetic field, the $|S\rangle$ state is typically the ground state and the three degenerate triplet states are higher in energy by the exchange energy J.[10] Since J scales with the wavefunction overlap between the two electrons, J is large in the $(0, 2)$ configuration and small in the $(1, 1)$ configuration.[11] This difference in exchange leads to a situation where although the forward $(1, 1) \rightarrow (0, 2)$ interdot transition is allowed for the $|S\rangle$ ground states, current does not flow. This occurs because, with $J(1,1) < J(0,2)$, it is possible that even though conduction through the singlet states is allowed, i.e., $\mu_{LL} \geq \mu_l^{|S\rangle}(1,1) \geq \mu_r^{|S\rangle}(0,2) \geq \mu_{RL}$, the interdot transition for the triplet states

a)Electronic mail: jperron@csusm.edu
b)Electronic mail: Neil.Zimmerman@nist.gov. Tel.: (301) 975-5887

 © 2016 AIP Publishing LLC

Reuse of AIP Publishing content is subject to the terms at: https://publishing.aip.org/authors/rights-and-permissions. Download to IP: 129.6.107.10 On: Fri, 08 Apr 2016 14:23:12

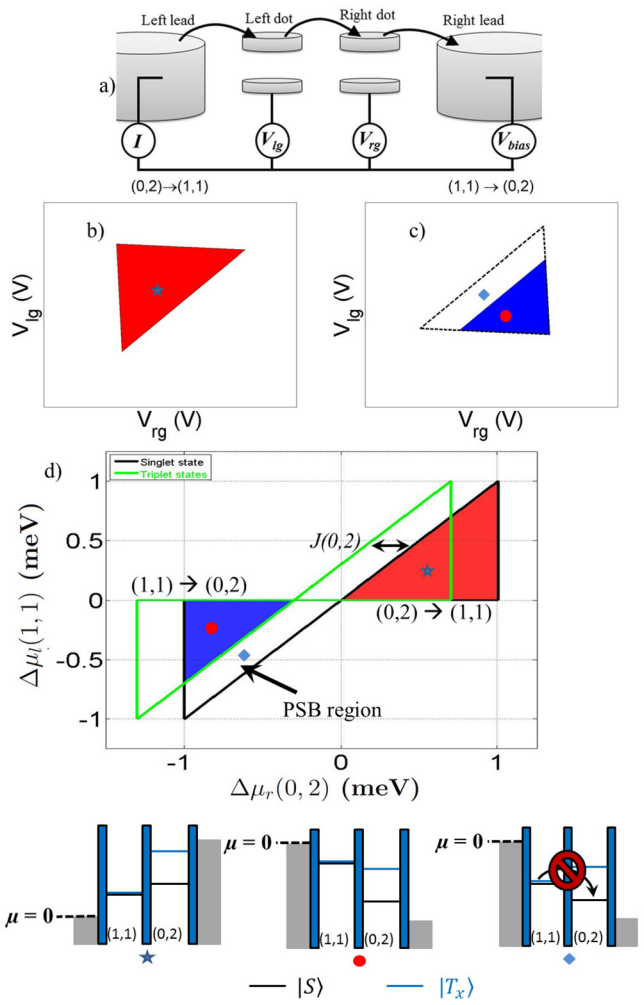


FIG. 1. Traditional forward Pauli-spin blockade, B = 0 T Bias triangles at the $(1,1) \leftrightarrow (0,2)$ charge transition with no applied magnetic field, $V_{bias} = \pm 1$ mV and $J(0,2) = 0.3$ meV. (a) Schematic of a typical double quantum dot. A bias applied between the left and right leads can lead to electrons tunneling through the device. The potentials of the dots are controlled with two capacitively coupled gates. (b) and (c) Voltage space pictures of current measurements in the (0, 2) → (1, 1) and (1, 1) → (0, 2) biasing directions using typical voltage and capacitance values. Filled regions of color correspond to non-zero current. (d) The chemical potential space picture for the same transitions. Triangles below the $\Delta\mu_l(1,1) = 0$ axis are for (1, 1) → (0, 2) biasing and those above are for (0, 2) → (1, 1) biasing. Chemical potential diagrams for certain regions of interest in (b)–(d) are also shown. The μ-space origin is determined by the Fermi level of the left lead which we take to be at the ground potential for all measurements. The PSB region is labelled with the blue diamond.

is forbidden, $\mu_l^{|T_x\rangle}(1,1) \leq \mu_r^{|T_x\rangle}(0,2)$. Thus, once loaded, the $|(1,1)T_x\rangle$ can tunnel neither forward nor back until it has relaxed into a singlet state. Since the spin relaxation from a $|T_x\rangle$ state to a $|S\rangle$ state is typically long relative to the tunneling times, the measured current in the PSB region is near or below the noise floor of the measurement system. This situation truncates the size of the bias triangles in the forward bias direction, as shown in Figure 1(c), while leaving the triangles measured in the reverse bias direction at "full size," as in Figure 1(b). This size difference is the most basic signature of PSB and has been measured by several groups in various material systems.[5,12–21]

For a more intuitive presentation of the voltage space measurements depicted in Figures 1(b) and 1(c), one can convert them to chemical potential space, or μ-space,[22] where triangles from both bias polarities can be shown on a single plot. Plotted in Figure 1(d) is the μ-space equivalent to what is shown in both panels (b) and (c), where the axes are defined as $\Delta\mu_l(1,1) \equiv \mu_l^{|S\rangle}(1,1) - \mu_{LL}$ and $\Delta\mu_r(0,2) \equiv \mu_r^{|S\rangle}(0,2) - \mu_{LL}$. Also shown in this plot are outlines of the "state triangles," which correspond to the conditions $\mu_{LL} \geq \mu_l^{state}(1,1) \geq \mu_r^{state}(0,2) \geq \mu_{RL}$, in the forward biased direction and $\mu_{RL} \geq \mu_r^{state}(0,2) \geq \mu_l^{state}(1,1) \geq \mu_{LL}$, with $\mu_{LL} \equiv 0$, in the reverse direction, where *state* refers to the spin state, $|S\rangle$ or $|T_x\rangle$, of the two electron system.

When a magnetic field, B, is applied, several effects can occur depending on the direction of the applied field. If applied perpendicular to the two-dimensional electron gas (2DEG), there can be a significant change in the spatial wavefunctions of the electrons. This will in turn affect the magnitudes of $J(1,1)$ and $J(0,2)$ leading to a change in size of the PSB region.[12] At higher fields, the $|T_x\rangle$ states can fall below the $|S\rangle$ states leading to PSB in the (1, 1) → (0, 2) direction caused by singlet states rather than the triplet states.[23] When B is applied in the plane of the 2DEG, the spatial effect on the wave functions is negligible and observed effects are due to the Zeeman splitting of the triplet levels. This in-plane magnetic field dependence will be the focus of the remainder of this manuscript.

When considering the in-plane B, we make the following assumptions for B-dependence of the chemical potentials:

$$\mu^{|S\rangle}(n,m)|_{B\neq 0} = \mu^{|S\rangle}(n,m)|_{B=0}, \tag{1}$$

$$\mu^{|T_0\rangle}(n,m)|_{B\neq 0} = \mu^{|S\rangle}(n,m)|_{B=0} + J(n,m), \tag{2}$$

$$\mu^{|T_\pm\rangle}(n,m)|_{B\neq 0} = \mu^{|S\rangle}(n,m)|_{B=0} + J(n,m) \pm g\mu_B B. \tag{3}$$

III. MAGNETIC FIELD DEPENDENCE

When B is increased from zero, the first notable effect is the change in size of the bias triangles. As reported in Ref. 13, the triangles in the forward (1, 1) → (0, 2) biasing direction grow in size proportional to the Zeeman energy $E_Z = g\mu_B B$, with g being the electron g-factor and μ_B being the Bohr magneton. However, we predict a concomitant reduction in size of the triangles measured in the reverse (0, 2) → (1, 1) direction. Both of these effects are illustrated in Figure 2.

Figure 2(a) shows the μ-space picture of the changing triangles (see the supplementary material[24] for details on using the μ-space picture to determine the regions of allowed current). The origin is defined by the point where $\mu_l^{|S\rangle}(1,1) = \mu_r^{|S\rangle}(0,2) = \mu_{LL} = 0$. Since $\mu^{|S\rangle}(n,m)$ has no magnetic field dependence, our definition of the origin relates it to a single point in voltage space, at all magnetic fields. This consistent mapping between μ-space and voltage space results in predictive power not available in the typical voltage space picture. Directions determined in μ-space now map to specific directions in voltage space across all magnetic fields. This allows us to predict, for example, the fact that bias triangles measured at low magnetic fields change size along the $\Delta\mu_l(1,1)$ direction, which maps to a voltage

Reuse of AIP Publishing content is subject to the terms at: https://publishing.aip.org/authors/rights-and-permissions. Download to IP: 129.6.107.10 On: Fri, 08 Apr 2016 14:23:12

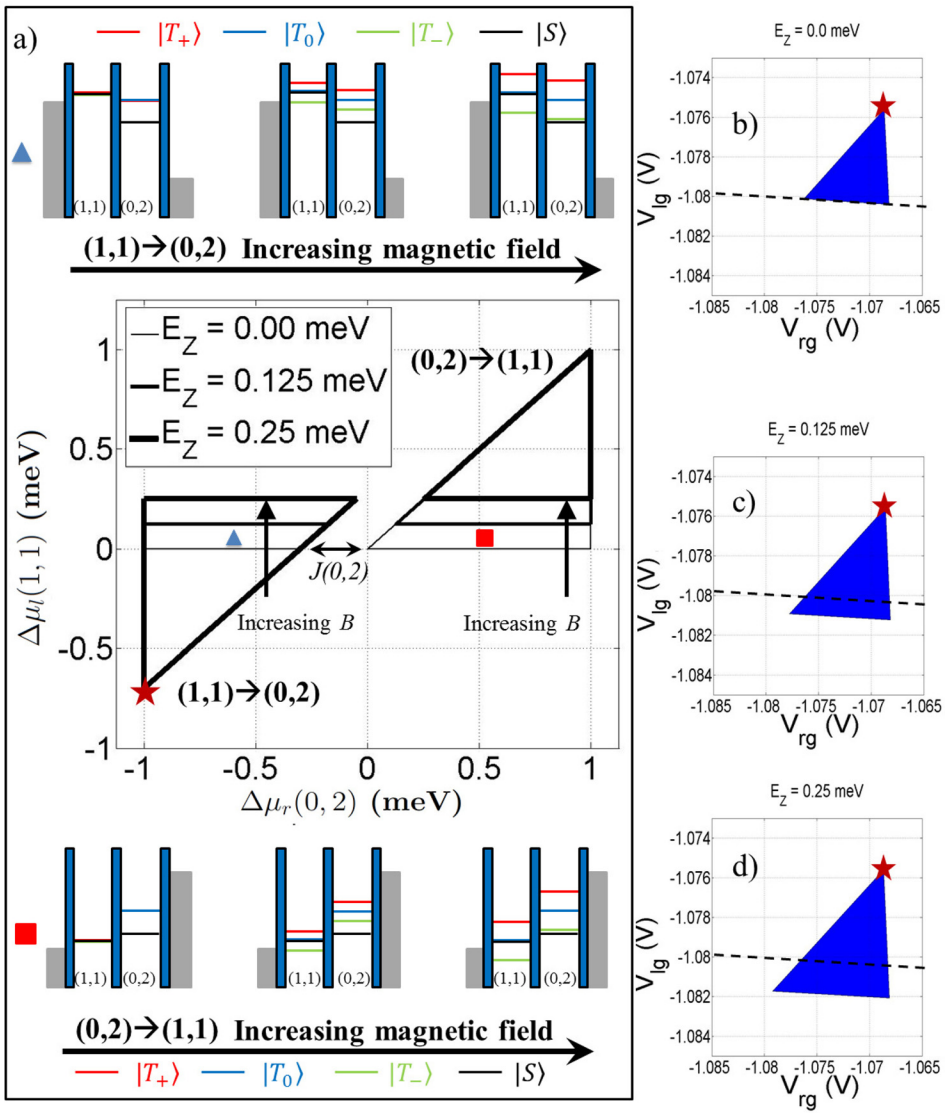


FIG. 2. Magnetic field dependence for $\mathbf{B} \leq \mathbf{B_{ST}}$: (a) μ-space picture of bias triangles in both biasing directions with $V_{bias} = \pm 1$ mV, $J(0, 2) = 0.3$ meV at three B values corresponding to $E_Z = 0.0$, 0.125, and 0.25 meV, respectively. The triangles outlined with consecutively thicker lines correspond to higher B. As B is increased, the triangles in the forward (1, 1) → (0, 2) direction (left set of triangles) grow along the $\mu_l(1, 1)$ direction while the reverse (0, 2) → (1, 1) biased triangles shrink in the same direction. The change in triangle size is due to the Zeeman splitting of the $|(1, 1)T_-\rangle$ level as shown in the chemical potential diagrams corresponding to the points labeled with the blue triangle and the red square, respectively. (b)–(d) Gate voltage space bias triangles in the forward (1, 1) → (0, 2) biasing direction at the same magnetic fields as (a). The vertex labeled with the star occurs at the same position at all magnetic fields in both μ-space and gate voltage space. The growth direction we predict is clear and agrees with the data in Figure 4 of Ref. 13.

space direction roughly along the V_{lg} axis (see Figure 2 and the discussion below).

The change in triangle size in the $\Delta\mu_l(1, 1)$ direction is understood by considering the process which determines the edge of the triangles. For the forward (1, 1) → (0, 2) direction, the crucial process is the loading of an electron from the left lead onto the left dot. As B is increased, the $|(1, 1)T_-\rangle$ level is lowered by the Zeeman energy meaning that the loading of that state can occur at larger $\Delta\mu_l(1, 1)$ values. This is shown in the chemical potential diagrams at the top of Figure 2(a) for the point labelled with the blue triangle. In this region, since the only accessible (1, 1) state is $|T_-\rangle$, conduction is spin-polarized. In the reverse (0, 2) → (1, 1) direction, the crucial process is the Coulomb blockade of current due to loading of the $|(1, 1)T_-\rangle$ level below μ_{LL}. Again, as B is increased this level drops below μ_{LL} at a higher $\Delta\mu_l(1, 1)$. This is depicted in the chemical potential diagrams at the bottom of Figure 2(a) for the point labeled with the red square. In both biasing directions, when viewed in this μ-space picture, the direction the triangles are changing is clear, and we can then easily generate the correct gate voltage space picture. This is done in Figures 2(b)–2(d), using typical capacitance and voltage parameters, which show bias triangles for the forward (1, 1) → (0, 2) direction growing with magnetic field in roughly the $-V_{lg}$ direction (as compared to the detuning direction, i.e., perpendicular to the base of the triangles). This prediction is observed in Ref. 13 and validates the assumptions made in Equations (1)–(3).

As B is increased further there will be a crossover from PSB in the forward (1, 1) → (0, 2) direction, as discussed above and in the previous works,[1,5,12–21,23,25] to PSB in the reverse (0, 2) → (1, 1) direction. The onset of this reverse PSB is accompanied by the development of a tail-like feature in the regions of allowed current[26] and occurs at a magnetic field B_{ST} where $E_Z = J(0, 2)$.

Both of the high field features can be understood by considering Figure 3, a μ-space picture of a transport measurement in the reverse (0, 2) → (1, 1) direction with $E_Z > J(0, 2)$. Included are the state triangles for the various singlet and triplet chemical potential levels. The regions labeled with the blue diamond and square correspond to the region of PSB. The physics of this PSB is similar to the traditional low field (1, 1) → (0, 2) PSB, but with the $|(0, 2)S\rangle$ state filling the role of the trapped state and the $|T_-\rangle$ levels contributing to current. This is shown in the corresponding chemical potential diagrams. Throughout the PSB region, although current

Reuse of AIP Publishing content is subject to the terms at: https://publishing.aip.org/authors/rights-and-permissions. Download to IP: 129.6.107.10 On: Fri, 08 Apr 2016 14:23:12

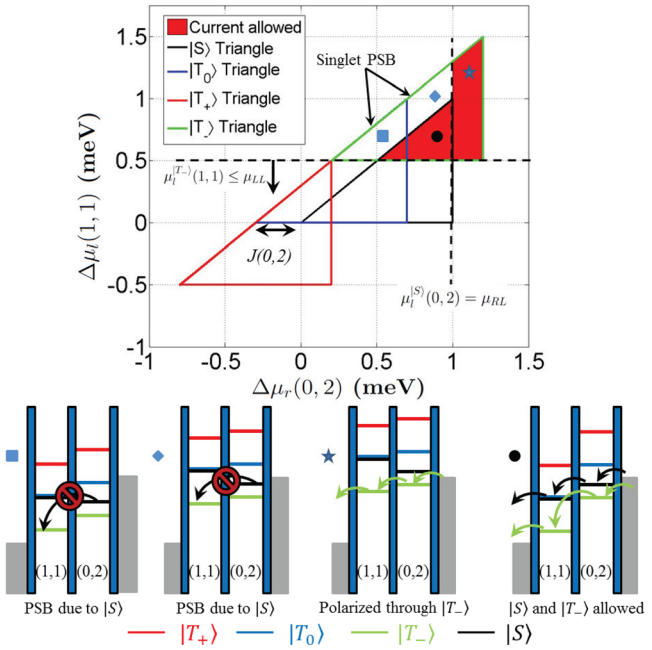


FIG. 3. $\mathbf{B} \geq \mathbf{B_{ST}}$ μ-space picture of transport in the reverse (0, 2) → (1, 1) direction with an applied magnetic field $g\mu_B B = 0.5$ meV, $J(0, 2) = 0.3$ meV and $V_{bias} = -1$ mV. The region of allowed current (red) is no longer triangular. The tail-like feature, indicated with the star, consists of current through only the $|T_-\rangle$ levels and therefore is a spin polarized current upon exiting the DQD. The regions identified with the diamond and square symbols define the area of PSB. Unlike the typical PSB, this high-field PSB is caused by the loading of the $|(0,2)S\rangle$ level rather than the $|(1,1)T\rangle$ level. This means that any leakage current measured in this region is due to relaxing from the $|(0,2)S\rangle$ and $|(0,2)T_-\rangle$ states. In the region identified by the black circle current is allowed through both the $|S\rangle$ and $|T_-\rangle$ states. Below the μ-space plot are chemical potential diagrams for the indicated positions with key transitions indicated with arrows.

is allowed through the ground state $|T_-\rangle$ levels, the $|(0,2)S\rangle$ state can load from the right lead and, since the $|(0,2)S\rangle \rightarrow |(1,1)T_-\rangle$ tunneling event is not allowed, it will block current until it relaxes to a $|T_-\rangle$ state. Much like how the leakage current in the low field (1, 1) → (0, 2) PSB region has been used to probe $|T\rangle \rightarrow |S\rangle$ coupling/relaxation, leakage currents in this reverse PSB region could be used to probe $|S\rangle \rightarrow |T\rangle$ relaxation.

Figure 3 has another distinct feature, the tail region labeled with the star. This feature also develops when the $|T_-\rangle$ state becomes the ground state in the (0, 2) configuration. The feature can be understood by considering the border between the tail and the PSB region. To the left of this border, no current is measured because the $|(0,2)S\rangle$ can load and prevent current flow as previously discussed. To the right of the border, the $|(0,2)S\rangle$ level is above μ_{RL} and is therefore unable to load (compare the chemical potential diagrams labelled with the diamond and the star). Since the $|(0,2)T_-\rangle$ state is the only state that can load, the current measured in the tail region will be spin polarized upon exiting the DQD, which suggests a potential use as a polarized spin current source.[27]

IV. CONCLUSIONS

By thoroughly considering the μ-space picture typically used to explain PSB, we have identified several interesting and unexplored features involved in the (1, 1) ↔ (0, 2) transition of a double quantum dot at both low and high magnetic fields. The boundary between the two field regimes occurs at B_{ST} where the Zeeman energy of $|(0,2)T_-\rangle$ equals $J(0, 2)$. With $g = 2$ and exchange energies reported[13,17,20] in the range of 0.24 meV–1.4 meV, B_{ST} in Si should be in the range of 2–12 T, accessible with standard cryomagnetics. This suggests that Si offers an opportunity to test our predictions. Simple validation can be achieved by performing measurements of the type reported in Ref. 13 for both biasing directions and comparing with our predictions of changing triangle size. Following that, the high-field tail feature we predict should be a clear signature that the reverse PSB regime has been reached, signaling a crossover in magnetic field to qualitatively different behavior. This would lead to a deeper understanding of transport through double quantum dots by providing several new comparisons between measurement and the standard theory.

ACKNOWLEDGMENTS

We are grateful for the many useful discussions with Josh Pomeroy, Garnett Bryant, Mark Stiles, and Michael Gullans.

[1]K. Ono, D. G. Austing, Y. Tokura, and S. Tarucha, Science **297**, 1313 (2002).
[2]J. R. Petta, A. C. Johnson, A. Yacoby, C. M. Marcus, M. P. Hanson, and A. C. Gossard, Phys. Rev. B **72**, 161301 (2005).
[3]Y. Hu, F. Kuemmeth, C. M. Lieber, and C. M. Marcus, Nat. Nano **7**, 47 (2012).
[4]A. C. Johnson, J. R. Petta, J. M. Taylor, A. Yacoby, M. D. Lukin, C. M. Marcus, M. P. Hanson, and A. C. Gossard, Nature **435**, 925 (2005).
[5]S. Nadj-Perge, S. M. Frolov, J. W. W. van Tilburg, J. Danon, Y. V. Nazarov, R. Algra, E. P. A. M. Bakkers, and L. P. Kouwenhoven, Phys. Rev. B **81**, 201305 (2010).
[6]J. R. Petta, A. C. Johnson, J. M. Taylor, E. A. Laird, A. Yacoby, M. D. Lukin, C. M. Marcus, M. P. Hanson, and A. C. Gossard, Science **309**, 2180 (2005).
[7]F. H. L. Koppens, C. Buizert, K. J. Tielrooij, I. T. Vink, K. C. Nowack, T. Meunier, L. P. Kouwenhoven, and L. M. K. Vandersypen, Nature **442**, 766 (2006).
[8]K. C. Nowack, F. H. L. Koppens, Y. V. Nazarov, and L. M. K. Vandersypen, Science **318**, 1430 (2007).
[9]W. G. van der Wiel, S. De Franceschi, J. M. Elzerman, T. Fujisawa, S. Tarucha, and L. P. Kouwenhoven, Rev. Mod. Phys. **75**, 1 (2002).
[10]N. W. Ashcroft and N. D. Mermin, *Solid State Physics* (Thomson Learning, 1976).
[11]In this paper, we take $J(1, 1) = 0$ for simplicity. Including a finite value would not significantly affect the results of this work.
[12]A. C. Johnson, J. R. Petta, C. M. Marcus, M. P. Hanson, and A. C. Gossard, Phys. Rev. B **72**, 165308 (2005).
[13]N. S. Lai, W. H. Lim, C. H. Yang, F. A. Zwanenburg, W. A. Coish, F. Qassemi, A. Morello, and A. S. Dzurak, Sci. Rep. **1**, 110 (2011).
[14]G. Yamahata, T. Kodera, H. O. H. Churchill, K. Uchida, C. M. Marcus, and S. Oda, Phys. Rev. B **86**, 115322 (2012).
[15]C. B. Simmons, T. S. Koh, N. Shaji, M. Thalakulam, L. J. Klein, H. Qin, H. Luo, D. E. Savage, M. G. Lagally, A. J. Rimberg, R. Joynt, R. Blick, M. Friesen, S. N. Coppersmith, and M. A. Eriksson, Phys. Rev. B **82**, 245312 (2010).
[16]F. H. L. Koppens, J. A. Folk, J. M. Elzerman, R. Hanson, L. H. W. van Beveren, I. T. Vink, H. P. Tranitz, W. Wegscheider, L. P. Kouwenhoven, and L. M. K. Vandersypen, Science **309**, 1346 (2005).
[17]N. Shaji, C. B. Simmons, M. Thalakulam, L. J. Klein, H. Qin, H. Luo, D. E. Savage, M. G. Lagally, A. J. Rimberg, R. Joynt, M. Friesen, R. H. Blick, S. N. Coppersmith, and M. A. Eriksson, Nat. Phys. **4**, 540 (2008).
[18]H. O. H. Churchill, A. J. Bestwich, J. W. Harlow, F. Kuemmeth, D. Marcos, C. H. Stwertka, S. K. Watson, and C. M. Marcus, Nat. Phys. **5**, 321 (2009).

Reuse of AIP Publishing content is subject to the terms at: https://publishing.aip.org/authors/rights-and-permissions. Download to IP: 129.6.107.10 On: Fri, 08 Apr 2016 14:23:12

[19]B. Weber, T. H. Matthias, S. Mahapatra, T. F. Watson, H. Ryu, R. Rahman, L. C. L. Hollenberg, G. Klimeck, and M. Y. Simmons, Nat. Nano **9**, 430 (2014).
[20]H. W. Liu, T. Fujisawa, Y. Ono, H. Inokawa, A. Fujiwara, K. Takashina, and Y. Hirayama, Phys. Rev. B **77**, 073310 (2008).
[21]A. Pfund, I. Shorubalko, K. Ensslin, and R. Leturcq, Phys. Rev. Lett. **99**, 036801 (2007).
[22]J. K. Perron, J. M. D. Stewart, and N. M. Zimmerman, J. Phys.: Condens. Matter **27**, 235302 (2015), specifically Equations (1) and (2).
[23]Y. C. Sun, S. Amaha, S. M. Huang, J. J. Lin, K. Kono, and K. Ono, Appl. Phys. Lett. **101**, 263108 (2012).
[24]See supplementary material at http://dx.doi.org/10.1063/1.4945393 for a description of how to use state triangles in μ-space to determine regions of allowed current.
[25]H. O. H. Churchill, F. Kuemmeth, J. W. Harlow, A. J. Bestwick, E. I. Rashba, K. Flensberg, C. H. Stwertka, T. Taychatanapat, S. K. Watson, and C. M. Marcus, Phys. Rev. Lett. **102**, 166802 (2009).
[26]These tail features are qualitatively similar to those associated with lifetime enhanced transport (LET)[15,17] but arise from very different physical mechanisms. In this work, the tail arises from energetically favorable tunneling events in equilibrium and does not depend at all on relative tunneling and relaxation rates. In contrast, LET arises from significant conduction through excited states and explicitly depends on appropriate ratios of tunneling rates and relaxation rates.
[27]The current is polarized upon exiting the double quantum dot, however, the spin relaxation process of the electrons once in the Fermi sea of the lead is likely to be fast, quickly diminishing the polarization of the current.

Reuse of AIP Publishing content is subject to the terms at: https://publishing.aip.org/authors/rights-and-permissions. Download to IP: 129.6.107.10 On: Fri, 08 Apr 2016 14:23:12